Uncertainty Set, Design and Performance Evaluation of Centralized Controllers for AMB System

Rafal P. Jastrzebski[1,a], Katja M. Hynynen[1,b], Alexander Smirnov[1,c]
[1]Dept. of Electrical Engineering, LUT Energy, Lappeenranta University of Technology,
PO 20, 53851 Lappeenranta, Finland
[a]rafal.jastrzebski@lut.fi, [b]katja.hynynen@lut.fi, [c]alexander.smirnov@lut.f

Abstract: In this paper an industrially recognized modal control approach, a linear-quadratic-Gaussian (LQG) control, and an H∞ control designs are compared using automated weights tuning based on a genetic algorithm. The robust stability analysis is carried out based on the uncertainty set, which comprises parametric and nonparametric uncertainties. The uncertainty set is updated to be compliant with the measured frequency responses of the test rig. The studied combination of the uncertainties proves too conservative for the direct application in the H∞ control synthesis. However, a robust stability of the controllers synthesized using the nominal plant can be verified using μ-analysis and the very uncertainty set that cannot be used for the controller design directly. It is demonstrated that for the rigid rotor without strong gyroscopic coupling all of the control approaches result in a similar performance. For the more slender rotor with an additional disc and the dynamics dependent on the rotational speed the best results are achieved by the LQG and H∞ controllers. When no gain scheduling is applied, the modal control results in the unstable system.

Keywords: Modal Control, H-Infinity Control, Optimal Control, Finite Element Analysis

Introduction

The literature provides a significant number of different linear control approaches when applied
to AMB systems. The most straightforward methods include PID type controllers applied locally for each bearing and separately for each bearing axis. Such a decentralized control can be used in some applications fulfilling the ISO standards [1]. However, the centralized control approaches provide higher performance capabilities [2], [3] and therefore they can be applied to the systems which could not safely operate with the simple controllers. This concerns the systems with a high gyroscopic coupling, high rotational speeds, operation in a supercritical region, and strong disturbance forces, which require high disturbance attenuation. With the centralized control approaches it is possible to better counter the effects of certain imperfect or trade-off hardware configurations such as: non-collocation, noisy measurements, reduced bias currents, low bearing capacities, and small clearances. With a rapid development of the semiconductor industry, the powerful digital signal processors and field programmable gate arrays are readily affordable and the lack of computational power is no longer a decisive issue in the control algorithm selection.

The literature relating to AMB control does not provide objective comparison between different centralized AMB control approaches. In particular, in [3], as the most feasible controllers are introduced a modal control and an H_∞ control. In [3], a linear quadratic Gaussian (LQG) control is criticized as the one that does not feature appreciable advantages over the modal control. A credible comparison between various control strategies is difficult because of different tuning approaches. Manual selection of tuning parameters yields, in fact, trial and error tuning. Lösch [4] provided a qualitative comparison of different AMB controller design methods based on a literature survey. Grega and Piłat [5] presented a comparison between two linear quadratic (LQ) controllers, which had hand-selected weighting matrices. Jastrzebski and Pollanen [2] compared the centralized linear quadratic

Gaussian (LQG) control with the decentralized PID and PI/PD structures. Most of the literature, which describes the robust control of AMB rotor systems, employs ad hoc formed uncertainties. Typically, the rotational speed is considered as an uncertain parameter [6]. Few studies analyzed in depth uncertainty specifications. Li et al. [7] applied *v* gap metric to analyze uncertainty propagation for AMB rotor systems.

The motivation behind this work is to compare the application of the different control approaches, such as the modal control (center of gravity control), LQG, and H_∞ control, to the AMB rotor system. Moreover, the feasibility of a detailed parametric and nonparametric uncertainty set in the design and verification of the AMB control is studied.

The paper is organized as follows. First, the AMB system and its nominal and uncertain models are introduced. Second, the different control design methods are discussed. Third, comparison of the controllers and analysis of the results are conducted. Finally, the conclusions and the outlook are given.

System Modeling

The case study AMB system is non-symmetric, current controlled, and non-collocated. The rotor is of a long rotor type, which does not exhibit a significant gyroscopic effect (Fig. 1a). The machine is subcritical. From the radial position control point of view, the measured outputs are rotor displacements in two axes in two sensor planes and the applied control signals are four control currents of two radial eight-pole magnetic bearings. The system parameters are presented in Table 1.

In order to have comprehensive comparison of the controllers we introduce a second case theoretical system. Namely, the finite element method (FEM) model (Fig. 2) of the first rotor is modified. The rotor is made more slender and the coupling with the high diameter disc is attached to one of the ends making the second rotor more flexible and more gyroscopic (Fig. 1b).

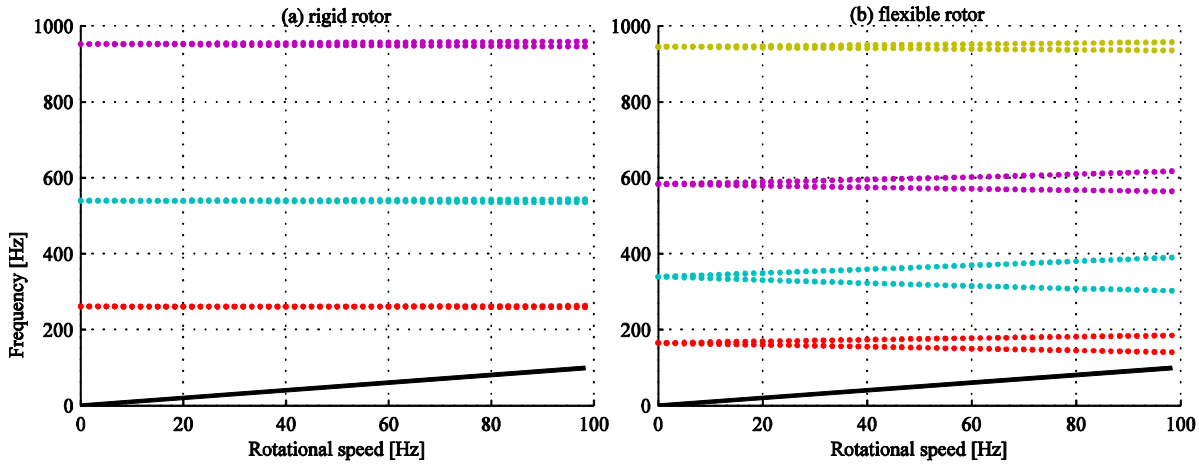

Figure 1: Campbell diagrams.

Table 1: Parameters of the case study systems

Parameter	Rigid rotor	Flexible rotor
Current stiffness and position stiffness	268 N/A and 992 N/mm	
Rotor mass	46.2 kg	46.7 kg
Rotor transverse moment of inertia	4.8 kg·m^2	6.41 kg·m^2
Rotor polar moment of inertia	0.041 kg·m^2	0.152 kg·m^2

Damping ratio of 1–3 flexible modes	0.0041, 0.0022, 0.0043
DC link voltage	150 V 300 V
Bias current and maximum currents	2.5 A and 10 A
Nominal magnetic air-gap length	0.6 mm
Bandwidth of the actuator	290 Hz
Sampling time and PWM delay	100 μs and 25 μs

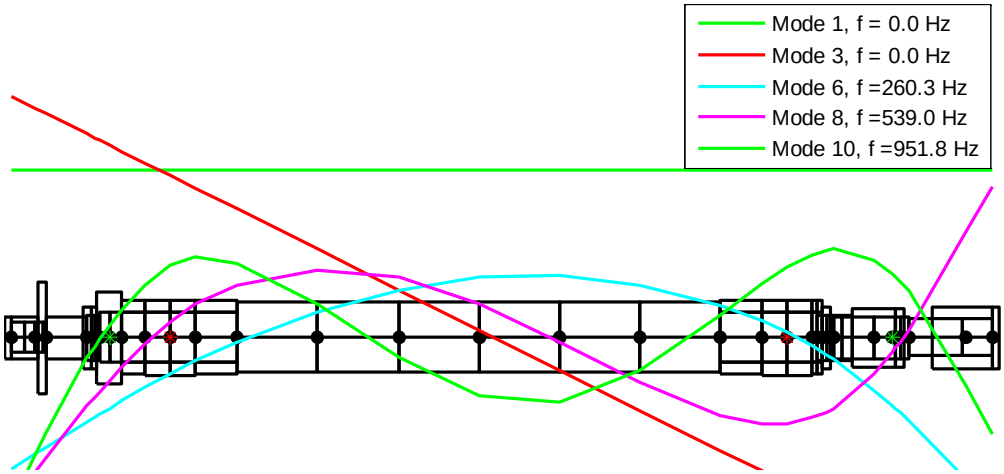

Figure 2: Rotor FEM model.

The AMB parameters remain the same for the both cases. In the second case, finding the controllers to stabilize the lightly damped bending modes is the significant challenge faced by the engineer. The stiffness-proportional damping is assumed. Damping ratio coefficients of the three bending modes are listed in Table 1.

For the model of the 1st physical system, the FEM model is tuned to better reflect the results of an experimental modal analysis of the free-free rotor [8] and results of frequency responses of the AMB levitated rotor. For each control input the actuator is modeled as a second order system with a pulse width modulation (PWM) delay and a motion-induced back electromotive force. The sensor model consists of third-order Pade rational approximations of sensor delays and sampling delays.

The nominal plant model, which is used for designing the modal controller, comprises the rigid rotor modes in the center of gravity coordinates and the first-order actuator model that has the same bandwidth as a more detailed actuator model. The sensors are modeled as gains. The nominal plant applied for the LQG control synthesis comprises the same rotor model but with the position stiffness and gyroscopic couplings and the first-order actuator model. The uncertain plant applied to H_∞ control synthesis comprises the rigid body mode, the first bending mode, uncertain rotational speed, and the first-order actuator. Finally, the plant model used for validation comprises the three rotor bending modes, the aforementioned detailed actuator model, and the detailed sensor model. It has additional outputs to monitor voltage commands and rotor displacements at the retainer bearings. The additional inputs for injecting disturbance forces are included.

The open-loop transfer function of the plant in the Laplace domain using the state-variable form can be written as

$$\mathbf{y} = \boldsymbol{G}(s)\mathbf{u} = \boldsymbol{C}(s\mathbf{I} - \boldsymbol{A})^{-1}\boldsymbol{B}\mathbf{u}. \quad (1)$$

$\boldsymbol{G}$(s) is a 4×4 transfer function matrix of the plant. **u** and **y** are the input vector and the output vector, respectively.

Uncertainty Set. The set of perturbed plants is constructed as a tool for the robust stability analysis and possibly control synthesis. The set is constructed using plant model, which includes the following parametric (structured) uncertainties:

- position stiffness (±20%) and the current stiffness (±10%)
- cross-coupled stiffness (±2% with respect to the current stiffness and ±4% with respect to the position stiffness)
- elements of the mass matrix (±2% for the parameters describing rigid body modes and ±3% for the parameters describing the first bending mode)
- damping of the first bending mode (±3%)
- sensor gains (±5%) and the location of sensors (±0.02m)
- electrical parameters (L: ±10%, R: ±10%).

The uncertain mode shape of the first bending mode is taken into account by introducing a perturbed location of the position sensors for that mode. According to the calculated force versus current characteristics of the studied radial bearings [9], the variations of the position stiffness are greater than the variations of the current stiffness as a function of the rotor position and the control current for the selected bias current. The uncertain cross-coupled stiffness and the uncertainty levels associated with the bending mode are based on suggestions provided by Li et al. [10]. The uncertainties in the modal damping and the modal mass of the first bending mode are adjusted to reflect the measured frequency responses of the test rig. The dynamic (frequency-dependent) uncertainties which result from the structural mode detected on frequency responses of the test rig are lumped into a multiplicative output uncertainty forming the perturbed plant

$$\boldsymbol{G}_{\mathrm{p}} = \left(\mathbf{I} + w_{\mathrm{o}}\boldsymbol{\Delta}_{\mathrm{o}}\right)\boldsymbol{G} \ , \ \left\|\boldsymbol{\Delta}_{\mathrm{o}}\right\|_{\infty} \le 1. \tag{2}$$

$w_{\mathrm{o}}(s)$ is a scalar weight such as $\left|w_{\mathrm{o}}(j\omega)\right| \ge l_{\mathrm{o}}(\omega)$ for each ω that

$$l_{\mathrm{o}}(\omega) = \max \bar{\sigma}\left(\left(\boldsymbol{G}_{\mathrm{p}} - \boldsymbol{G}\right)\boldsymbol{G}^{-1}(j\omega)\right), \tag{3}$$

where $\left\|.\right\|_{\infty}$ and $\bar{\sigma}(.)$ denote the H_{∞} norm and the maximum singular value, respectively. Similarly, the uncertainty can be added as an input multiplicative one. Fig. 3. presents the frequency responses of the corresponding uncertainty models, that is, the values of $l_{\mathrm{o}}(\omega)$ and of $l_{\mathrm{i}}(\omega)$. They are computed by searching through a set of 100 perturbed plants. In Fig. 3. we can see that the measured relative differences between the frequency responses and the nominal plant are below the analytically computed values of $l_{\mathrm{o}}(\omega)$ and $l_{\mathrm{i}}(\omega)$. Therefore, the uncertainty set is feasible for the robust stability analysis of the closed-loop control systems.

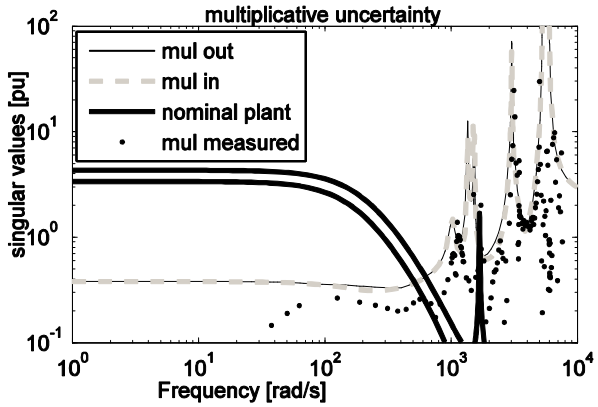

Figure 3: Maximum and minimum singular values of the nominal plant. The measured relative differences between the frequency responses of the test rig and the nominal plant model are compared to the differences obtained using the uncertainty set.

Control Synthesis

The traditional weighting in the LQG and the signal-based H_∞ control schemes [11] includes the weighing of the system inputs and outputs according to the expected relative signal importance and frequency content. The selection of the suitable weights is not a trivial task. In this work we apply a basic genetic algorithm (GA) to automate the control design based on the following control design objectives: output sensitivity peek, input and output disturbance attenuations, responses to the step disturbance and step reference position, testing physical limitations for state variables (voltage saturation, clearance), and system bandwidth. The LQG and the signal-based H_∞ control used in this work are related. The applied modal control also uses the LQG approach.

H-inf Control. In the general linear H_∞ problem the goal is to find an admissible controller $\boldsymbol{K}$, if one exists, so that for $\gamma>0$

$$\left\|\boldsymbol{F}_{\mathrm{l}}\left(\boldsymbol{P},\boldsymbol{K}\right)\right\|_\infty = \max_\omega \bar{\sigma}\left(\boldsymbol{F}_{\mathrm{l}}\left(\boldsymbol{P},\boldsymbol{K}\right)\left(j\omega\right)\right) \le \gamma\,. \tag{4}$$

Where $\boldsymbol{F}_{\mathrm{l}}$ is a lower fractional transformation equal to the closed-loop transfer function of the system presented in Fig 4a. $\bar{\sigma}$ is an upper singular value. The generalized plant $\boldsymbol{P}$ is obtained by augmenting the signal weighting functions to the original plant. Additionally, the inputs and outputs that correspond to the uncertain speed are also included. This way the structured uncertainty is introduced to the system by a block $\boldsymbol{\Delta}$ presented in Fig. 4b. The signal weights $\boldsymbol{W}_{\mathrm{d}}(s)$, $\boldsymbol{W}_{\mathrm{n}}(s)$, $\boldsymbol{W}_{\mathrm{i}}(s)$, $\boldsymbol{W}_{\mathrm{u}}(s)$, $\boldsymbol{W}_{\mathrm{e}}(s)$, and the weight for the reference tracking $\boldsymbol{W}_{\mathrm{ref}}(s)$ are of the form

$$\boldsymbol{W}(s) = \mathbf{I}_{4\times4}\,\frac{a_1 s + a_2 a_3}{s + a_3}\ . \tag{5}$$

The state weight matrix $\boldsymbol{W}_{\mathrm{s}}$ is in the form of a diagonal constant matrix, but for the signal-based H_∞ control problem it is left out from the scheme $\boldsymbol{W}_{\mathrm{s}}=\mathbf{0}$. The other than the rotational speed uncertain parameters can be also included into the $\boldsymbol{\Delta}$-structure, but the combination of too many uncertain parameters leads to the conservative uncertainty representation. Such an uncertainty set is not feasible for the synthesis of the practical controllers.

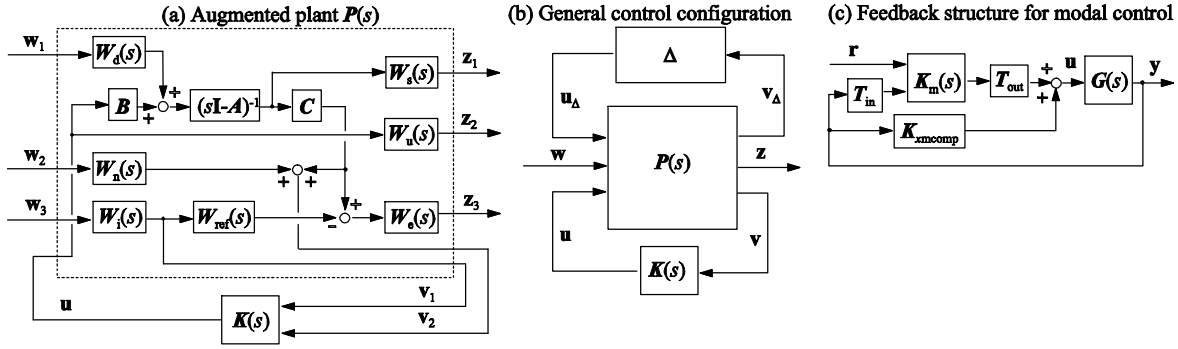

Figure 4: (a) 2 degrees-of-freedom H_∞ signal-based design problem. The vectors $\mathbf{w}_1$, $\mathbf{w}_2$, and $\mathbf{w}_3$ comprise the input distortion signals, the output distortion signals, and the reference signals, respectively. The vectors $\mathbf{v}_1$ and $\mathbf{v}_2$ are the weighted position reference signals $\mathbf{w}_3$ and the distorted sensor measurements, respectively. The vectors $\mathbf{z}_1$ and $\mathbf{z}_2$ consist of the weighted system input signals and the weighted position error signals, respectively.
(b) General control configuration. (c) Modal control. $\mathbf{r}$ is the vector of the reference modal positions.

LQG Control. The LQG problem can be cast as an H_2 problem to the general control configuration (Fig. 4a). The weighting matrices become the constant diagonal matrices of the design parameters $\boldsymbol{W}_\mathrm{d}=\boldsymbol{R}_w^{1/2}$, $\boldsymbol{W}_\mathrm{n}=\boldsymbol{R}_\mathrm{v}^{1/2}$, $\boldsymbol{W}_\mathrm{i}=\mathbf{0}$, $\boldsymbol{W}_\mathrm{u}=\boldsymbol{R}^{1/2}$, $\boldsymbol{W}_\mathrm{e}=\mathbf{0}$ and $\boldsymbol{W}_\mathrm{s}=\boldsymbol{Q}_1^{1/2}$. $\boldsymbol{R}_w$ is the process noise intensity or covariance matrix. $\boldsymbol{R}_\mathrm{v}$ is measurement noise intensity or covariance matrix. $\boldsymbol{R}$ and $\boldsymbol{Q}_1$ are the control weighting matrix and the state weighting matrix. For the LQG and for the modal control an input vector of reference signals $\mathbf{r}$ is added to the first-order compensator forming 2 degrees-of-freedom controllers.

Modal Control. In the case of the modal control the controller variables are in the center of gravity coordinates. The input and output signals are transformed in such a way that the plant appears to be decoupled and each mode can be controlled separately [3]. The gyroscopic term is also left out from the plant model. For the unsymmetrical systems the decoupling is not ideal and the control requires a compensation for the off-diagonal terms in the negative position stiffness matrix

$$\boldsymbol{K}_{x\mathrm{mcomp}} = \boldsymbol{K}_i^{-1}\boldsymbol{B}^{-1}\boldsymbol{K}_{x\mathrm{md}}\boldsymbol{C}^{-1} = \boldsymbol{T}_\mathrm{out}\boldsymbol{K}_{x\mathrm{md}}\boldsymbol{T}_\mathrm{in}\,, \tag{6}$$

where $\boldsymbol{T}_\mathrm{out}$ and $\boldsymbol{T}_\mathrm{in}$ are the transformation matrices applied to the outputs and to the inputs of the controller introduced with the positive feedback. $\boldsymbol{K}_{x\mathrm{md}}$ is the bearing stiffness matrix in the center of gravity coordinates that contains only the off-diagonal terms. In the resulting system, we can independently design a controller for the each mode. This is carried out by LQG control method. That way, it is possible to include an additional compensation of the gyroscopic coupling in the very same fashion as the off-diagonal stiffness compensation using the estimated velocities. The effective compensation can be realized when the number of sensors and actuators equals to the number of controlled modes. However, the compensation is not perfect because of the actuator and because of other differences between the ideal and the physical plant. Non-perfect compensation can be verified by the following inequality

$$\boldsymbol{T}_\mathrm{in}^{-1}\boldsymbol{G}_\mathrm{m}\boldsymbol{T}_\mathrm{out}^{-1}\left(\mathbf{I}+\boldsymbol{K}_{x\mathrm{comp}}\boldsymbol{T}_\mathrm{in}^{-1}\boldsymbol{G}_\mathrm{m}\boldsymbol{T}_\mathrm{out}^{-1}\right)^{-1} \neq \boldsymbol{G}\,, \tag{7}$$

where $\boldsymbol{G}_\mathrm{m}$ is the ideal plant model in the center of gravity coordinates and $\boldsymbol{G}$ includes the actuator dynamics.

Objective Tuning Using the Genetic Algorithm. The problem of credible comparison between the different control approaches and objective tuning can be alleviated by GA [2,12]. The GA searches for an optimal set of parameters of design weights taking into account the norms of the specified closed-loop transfer functions and time responses. The cost function (fitness function) that maps the chromosomes into the fitness values has multiple performance indices p_n:

- Minimize the sensitivity peak $M_S = \left\| \boldsymbol{S}_o \right\|_\infty$.
- Provide a high controller gain (a small maximum singular value of the sensitivity) at low frequencies $M_{SDC} = \overline{\sigma}\left(\boldsymbol{S}_o(\omega)\right)$, where $\omega \to 0$.
- Provide a sufficient input disturbance attenuation (maximize the tolerated disturbance forces) $M_{Ti} = \left\| \boldsymbol{K}_{fb}\boldsymbol{G}\boldsymbol{S}_i \quad \boldsymbol{G}\boldsymbol{S}_i \right\|_\infty$.
- Provide a sufficient output disturbance attenuation (maximize the tolerated errors in the measured displacements) $M_{To} = \left\| \boldsymbol{G}\boldsymbol{K}_{fb}\boldsymbol{S}_o \quad \boldsymbol{K}_{fb}\boldsymbol{S}_o \right\|_\infty$ and check weather the physical system limits (DC link voltage, clearances, control currents) are not violated.
- Minimize the value of γ in the case of an H_∞ controller.
- Minimize the overshoot in the case of the step response for the reference signal; and provide required rise time.
- Minimize signals amplitudes because of the step response for the disturbance force signal.

$\boldsymbol{K}_{fb}$ is the feedback path of the controller. The input sensitivity $\boldsymbol{S}_i = \left(\mathbf{I} + \boldsymbol{K}_{fb}\boldsymbol{G}\right)^{-1}$ and the output sensitivity $\boldsymbol{S}_o = \left(\mathbf{I} + \boldsymbol{G}\boldsymbol{K}_{fb}\right)^{-1}$. The output complementary sensitivity $\boldsymbol{T}_o = \boldsymbol{G}\boldsymbol{K}_{fb}\boldsymbol{S}_o$. The cost function is obtained as follows. First, the performance indices are evaluated using the accurate validation plant model. Second, the performance indices are used to calculate the corresponding normalized objective functions f_n. Third, each objective function is multiplied by the predefined weight w_n, and they are added together resulting in the single cost function

$$f = \sum_{n=1}^{N} w_n f_n \,, \tag{8}$$

where N equals to the number of the objective functions. The mating is carried out by the means of mutation, uniform crossover, and blending. The mutation rate is 40%. The optimal design is obtained after 40 iterations. The population size of the new synthesized controllers in the each iteration is 30.

Comparison of Controllers

The closed-loop feedback systems are evaluated using a more accurate plant model and the uncertainty set of the perturbed plants. The H_∞ control is synthesized using the uncertain speed where the nominal value is in the middle of the uncertainty range. The modal and LQG controllers are synthesized for zero rotational speed. Table 2 presents the results of the nominal and robust stability of the closed-loop control systems. The robust stability is evaluated for the nominal speed ±5 Hz (no brackets) and again for the uncertain speed from 0 to 100 Hz (information in the brackets). The robust stability for an uncertain system is computed using Matlab's robuststab command.

The calculated frequency response functions for the rigid rotor are presented in Figs. 5-6. The calculated frequency response functions for the flexible rotor are presented in Figs. 6-7. The sensitivity functions are evaluated at each operational point from 0 to 100 Hz and a maximum is calculated using the whole frequency spectrum for each point. The weighted unbalance responses are calculated for 100 g·mm coupled unbalance. The unbalance response and the weighted sensor disturbance response are calculated for the displacement limit on the safety bearings that equals to the half of the clearance, the control current limit that equals to the maximum control current (7.5 A) and the voltage command limit that equals to the DC link voltage. It is evident that such an unbalance is insignificant for the tested rotors. The greater concern is the periodical sensor disturbance that can result from a rotor run out or erroneous offsets in the position sensors. The values are calculated assuming the measured position errors equal to 5% of the airgap (30 μm).

In the case of the rigid rotor, the compensation of the off-diagonal stiffness in the modal control improves slightly the frequency responses. This improvement can be considerably greater when crossing the critical speed compared to the non-compensated control. The improvement is mostly because of the compensation of the off-diagonal stiffness. Adding the compensation of the gyroscopic matrix, as it is described in the Control Synthesis section, brings only the marginal improvement over the non-compensated control. The step responses when applying the disturbance force to one of the axis at the one of the radial bearings at the nominal speed are similar for all of the controllers because of the GA tuning.

In the case of the flexible rotor all the controllers are not robustly stable in the whole range of the rotational speed. The modal controller looses its nominal stability for the rotational speeds above 92 Hz. When applying a gain scheduling (GS) the controllers are robustly stable when within their respective speed ranges for the speed from 0 rpm to 10k rpm. However, the switching between the controllers can be problematic because of different steady state gains of the GA tuned controllers. This can be overcome by a bumpless transfer scheme [13] or by an interpolation. The H_∞ controllers are tuned for 14 rotational speed ranges and the plant model applied for the control design comprises the first and the second bending modes. It can be seen in Fig 7d that some of the controllers require more design iterations in order to decrease the sensitivity peak.

Table 2: Stability of the studied control systems.

Controller	**Stability of the rigid rotor system**		**Stability of the flexible rotor system**	
	Nominal	**Robust**	**Nominal**	**Robust**
H_∞	yes – full range	yes (yes)	yes – full range	yes (no)
H_∞ GS			yes – full range	yes
LQG	yes – full range	yes (yes)	yes – full range	yes (no)
modal	yes – full range	yes (yes)	yes – from 0 to 92 Hz	yes (no)

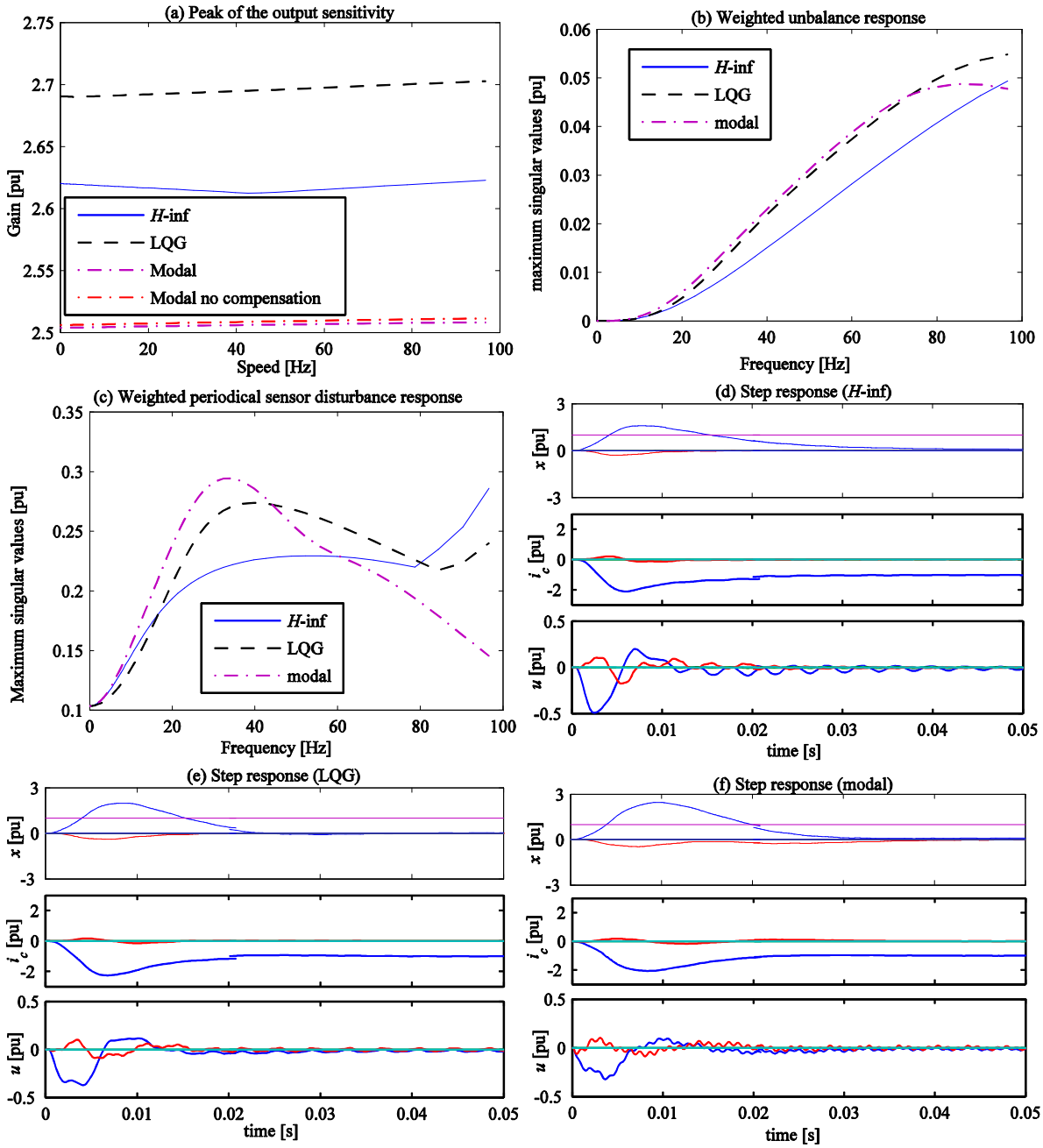

Figure 5: Evaluation of the different controllers for the rigid rotor system.

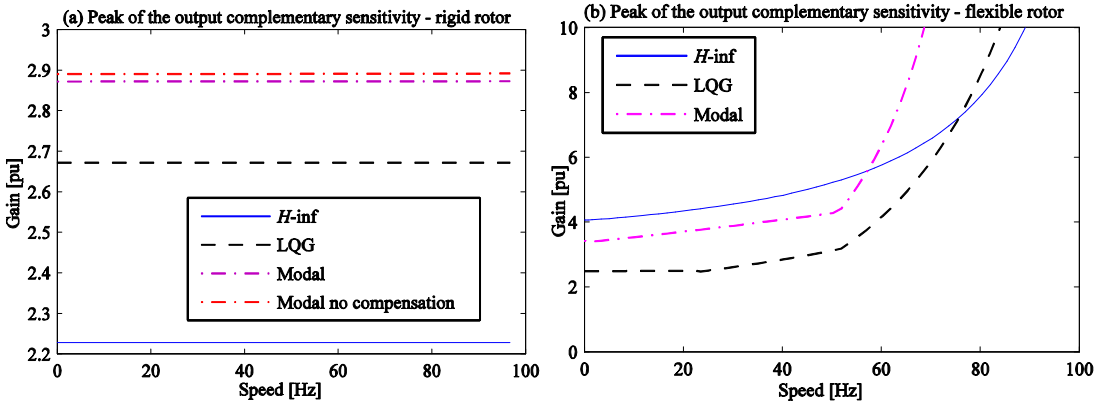

Figure 6: Output complementary sensitivity.

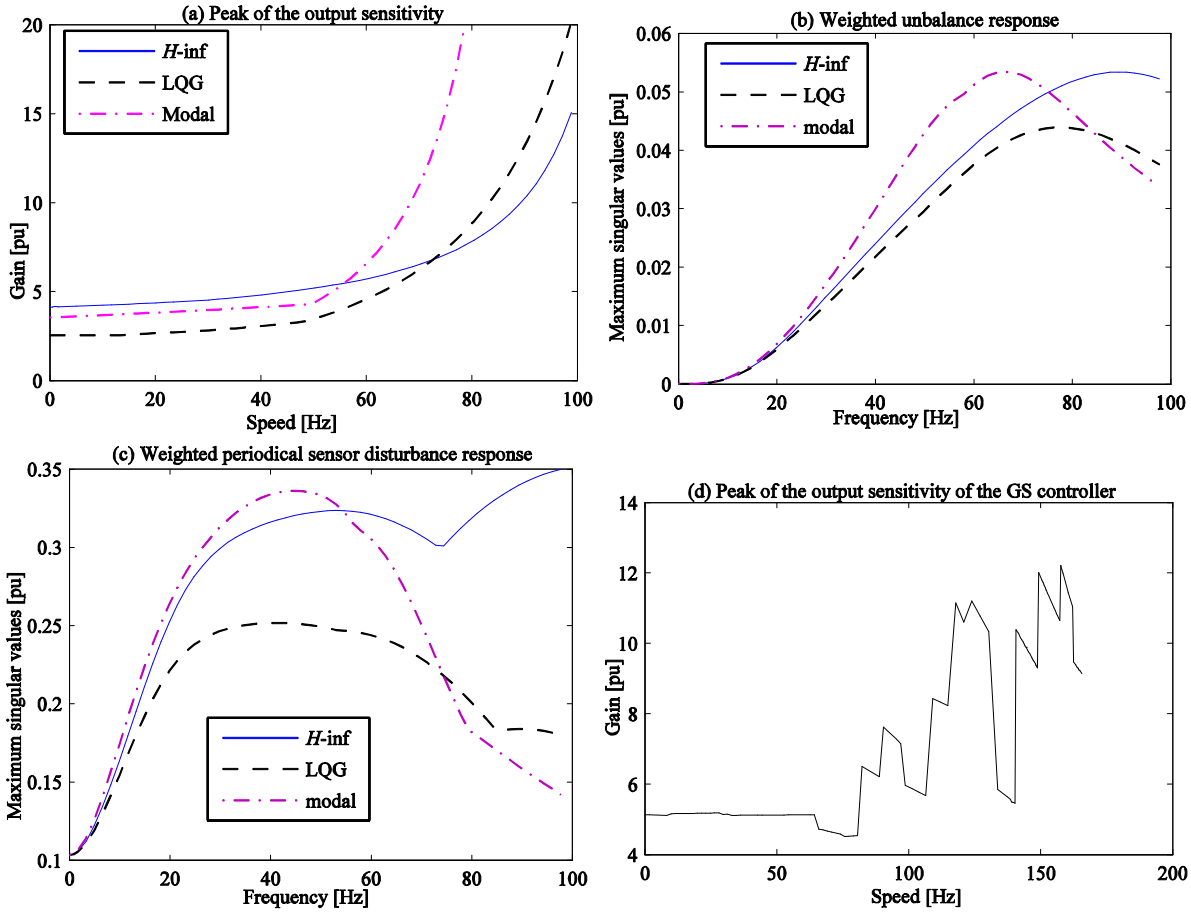

Figure 7: Evaluation of the different controllers for the flexible rotor system.

Conclusions

The comparison of the different centralized controllers was carried out for two different AMB rotor systems. It was shown that for the studied rotors there are no significant differences between the modal control, the LQG control and the H_∞ control methods when the GA-based tuning is applied. The H_∞ control provides the best results in terms of the frequency and time responses, but it is also the most costly solution for the digital implementation.

The modal control is limited by the hardware configuration. The control of the flexible modes cannot be achieved in the traditional AMB system with the two radial bearings. Moreover, the perfect decoupling and compensation of the off-diagonal terms of the bearing position stiffness matrix is not possible in the non-ideal system. The compensation of the gyroscopic term is also limited as it has to rely on the estimator of the velocities when only the position signals are available. For the studied systems, the most important advantage of the modal control is a less computationally intensive implementation than in the case of the centralized LQG and H_∞ control.

It was shown that the detailed uncertainty set can sufficiently capture the plant uncertainties and for that reason it can be used for the robust stability analysis. However, the combination of the many uncertainties proved to be too conservative for the practical H_∞ control synthesis.

For the studied flexible rotor AMB system the robust control when using the constant parameters of the controllers in the whole speed range was not achieved. The robust control with a non-adaptive controller could be still possible for the relaxed performance objectives in the GA tuning of that controller.

When the control of the flexible and gyroscopic rotors is required, the LQG and H_∞ control methods could benefit from adaptive control schemes. The GS H_∞ control provided robustly stable system in the speed range where it was not achievable by the controller with the constant parameters.

References

[1] N. Takahashi, H. Fujiwara, O. Matsushita, M. Ito, and Y. Fukushima, An evaluation of stability indices using sensitivity functions for active magnetic bearing supported high-speed rotor, Transactions of the ASME, Journal of Vibration and Acoustics Vol. 129 No. 2, pp. 230–238, 2007.

[2] R. P. Jastrzebski and R. Pollanen, Centralized optimal position control for active magnetic bearings: comparison with decentralized control, Electrical Engineering, Vol. 91, No. 2, pp. 101–114, 2009.

[3] G. Schweitzer and E.H. Maslen, Editors, Magnetic Bearings: Theory, Design, and Application to Rotating Machinery, Springer, New York, 2009.

[4] Lösch F, Identification and automated control design for active magnetic bearing systems. Dissertation, Swiss Federal Institute of Technology, Zurich, Switzerland, 2002.

[5] W. Grega, A. Pilat, Comparison of linear control methods for an AMB system. International Journal of Applied Mathematics and Computer Science, Vol. 15, No. 2, pp.245–255, 2005.

[6] S. Dietz, Robust Control Against Disturbance Model Uncertainty in Active Magnetic Bearings, in Proc. of 11th International Symposium on Magnetic Bearings, 2008.

[7] G. Li, Z. Lin, and P.E. Allaire, Uncertainty Classification of Rotor-AMB Systems, in Proc. of 11th International Symposium on Magnetic Bearings, 2006.

[8] R. Jastrzebski, R. Pöllänen, O. Pyrhönen, A. Kärkkäinen, J. Sopanen, Modeling and Implementation of Active Magnetic Bearing Rotor System for FPGA-based Control, in Proc. of 10th International Symposium on Magnetic Bearings, 2006.

[9] J. Nerg, R. Pöllänen, J. Pyrhönen, Modelling the force versus current characteristics, linearized parameters and dynamic inductance of radial active magnetic bearings using different numerical calculation methods, WSEAS Transactions on Circuits and Systems, Vol. 4, No. 6, pp. 551–559, 2005.

[10] G. Li, E.H. Maslen, P.E. Allaire, A note on ISO AMB stability margin, in Proc. of 10th International Symposium on Magnetic Bearings, 2006.

[11] S. Skogestad and I. Postlethwaite, Multivariable Feedback Control Analysis and Design, 2nd ed., Wiley, England, 2005.

[12] R.P. Jastrzebski, K. Hynynen, and A. Smirnov, H-infinity control of active magnetic suspension, Mechanical Systems and Signal Processing, Vol. 24, No. 4, pp. 995–1006, 2010.

[13] M. C. Turner and D. J. Walker, Linear quadratic bumpless transfer, Automatica, Vol. 36, No. 8, pp. 1089–1101, 2000.